J. Appl. Comput. Mech., 5(4) (2019) 652-666
DOI: 10.22055/JACM.2018.26787.1357

ISSN: 2383-4536
jacm.scu.ac.ir

M&MoCS

Shahid Chamran University of Ahvaz

Journal of Applied and Computational Mechanics

Research Paper

Impact of Magnetic Field on Convective Flow of a Micropolar Fluid with two Parallel Heat Sources

K. Periyadurai[1], M. Muthtamilselvan[2], Deog-Hee Doh[3]

[1] Department of Mathematics, Hindustan Institute of Technology and Science, Chennai - 603 103, India, Email: kperiyadurai@gmail.com

[2] Department of Mathematics, Bharathiar University, Coimbatore – 641 046, India, Email: muthtamil1@buc.edu.in

[3] Division of Mechanical Engineering College of Engineering, Korea Maritime and Ocean University
Busan - 49112, South Korea, Email: doh@kmou.ac.kr

Received August 16 2018; Revised November 10 2018; Accepted for publication November 15 2018.
Corresponding author: M. Muthtamilselvan, muthtamil1@buc.edu.in

Abstract. A numerical study is performed to analysis the buoyancy convection induced by the parallel heated baffles in an inclined square cavity. The two side walls of the cavity are maintained at a constant temperature. A uniformly thin heated plate is placed at the centre of the cavity. The horizontal top and bottom walls are adiabatic. Numerical solutions of governing equations are obtained using the finite volume method coupled with the upwind and central difference technique. Numerical results of the two-dimensional flow field governed by the Navier-Stokes equations are obtained over a wide range of physical parameters, namely the Rayleigh number, the Hartmann number, the inclined angle of the magnetic parameter and the vortex viscosity parameter. It is observed from the results, the heat transfer rate is reduced when increasing Hartmann number, inclination angle and vortex viscosity parameter. The higher heat transfer rate is obtained based on the Newtonian fluid compared to the micropolar fluid.

Keywords: Micropolar fluids; Numerical simulation; Magnetic field; Parallel plates.

1. Introduction

During the last several decades, free convective heat transfer in an inclined magnetic field has received great attention due to wide range of applications of the subject in the engineering, such as metallurgical melting, liquid metal, etc. Natural convection flow in a tilted cavity with magnetic field was studied by Al-Najem et al. [1]. They observed that the magnetic field effect is negligible in the heat transfer rate for the smaller values of the inclination angles. Ece and Buyuk [2] analyzed the MHD natural convection flow in an inclined enclosure. They revealed that the magnetic field suppresses flow intensity and heat transfer rate. The effect of an inclined magnetic field on natural convection in a cavity was investigated by Jalil and Al-Taey [3]. They concluded that the heat transfer rate decreases with the increase in the Hartmann number. Pirmohammadi and Ghassemi [4] numerically investigated the effect of transverse magnetic field on natural convection flow in a tilted enclosure and found out that the magnetic field strength increases, the convection is suppressed and hence the heat transfer rate is decreased. Teamah et al. [5] studied numerically natural convective flow for the combined buoyancy effects of thermal and mass diffusion in an inclined rectangular enclosure. They showed that the heat transfer mechanism reduces within the enclosure due to the retardation effect of the magnetic field. Sivaraj and Sheremet [6] have discussed free convection in an inclined porous cavity placed with a heat conducting body in the presence of magnetic field. Observation indicates that magnetic field decreases the fluid flow and reduces heat transfer rate.

Natural convection in a cavity induced by internal heat sources has concerned many researchers, due to its practical engineering applications, such as exchange of heat between building and environment, heat removal from electrical and

Published online: May 01 2019

electronic equipments, nuclear reactor design and control of flows in rooms due to thermal energy sources. Jetli et. al [7] conducted a numerical study on the influence of baffle location on natural convection in a partially divided enclosure. At high Rayleigh numbers, the tendency shows that the convection flow and average Nusselt number decreases with the increasing baffle conductivity. Natural convection heat transfer in a square cavity with a heated plate built in vertically as well as horizontally was studied by Oztop et. al [8]. They showed that the heat transfer rate is increased at both vertical and horizontal position of the plate as Grashof number increases. Kandaswamy et. al [9] analyzed the buoyancy convection in a square cavity in the presence of heated plate numerically. The overall heat transfer increased with the higher values of baffle-cavity ratios. The heat transfer is more enhanced in vertical direction than the horizontal direction. Garoosi et al. [10] utilized the Eulerian-Lagrangian to study solid particle behaviour on the fluid flow and heat transfer in an enclosure placed with heaters and coolers. Their results indicated that the fluid flow and heat transfer rate is strongly affected by the heaters and coolers in the entire cavity.

The theory of micropolar fluid was described by Eringen [11, 12] has been popular area of research in recent years. It is expected to describe successfully the non-Newtonian behaviour of certain fluids, such as liquid crystals, ferroliquids, colloidal fluids, and liquid with polymer additives. A numerical simulation on free convection of micropolar fluid in a partially divided cavity was performed by Wang et al. [13]. They reported that the vortex viscosity influences the flow field and heat transfer rate significantly. Zadravec et al. [14] performed a research on the natural convection of an enclosure with micropolar fluid and concluded that the micro-rotation of particles in fluid flow decreases the heat transfer rate significantly. Alloui et al. [15] have studied double-diffusive heat transfer of micropolar fluid in a vertical channel with Soret effects. It has been revealed that the fluid velocity profiles are very sensitive to the vortex viscosity parameter and fluid velocity decreases with the vortex viscosity parameter. A numerical study on MHD natural convection of micropolar fluids within square cavity has been considered for centrally located heat source by Muthtamilselvan et al., [16, 17]. The authors show that heat transfer rate of micropolar fluid is reduced by the inclined magnetic field and smaller than that of Newtonian fluid. Gibanov et al. [18] have investigated the natural convective flow of micropolar fluid in a trapezoidal cavity. This study shows that the convective flow and heat transfer rate are decreased with the high vortex viscosity parameter in the entire cavity. Convection heat transfer of micropolar fluid in a porous stretching sheet and heated/cooled deformable plate have been studied by Turkyilmazoglu [19, 20]. It is found that material parameter decreases the heat transfer rate. Also the convection effect is controlled by the magneto-convection parameter. Sheremet et al. [21] studied natural convection micropolar fluid in a wavy triangular enclosure. They reported that an increase in the vortex viscosity parameter suppresses heat transfer and fluid flow.

Based on the literature reviews, a large number of mathematical studies on natural convective heat transfer in the various types of cavities with different boundary conditions were examined. In this paper, a numerical study of MHD natural convection flow in a micropolar fluid in an inclined enclosure in the presence of parallel baffles has been performed. The effects of Rayleigh number, Hartmann number, and inclination angle on the flow and heat transfer characteristics have been examined.

2. Mathematical Formulation

The physical configuration of a system under consideration is a two dimensional inclined square cavity of length L as shown in Fig. 1. The vertical side walls of the cavity are isothermally maintained at a constant temperature T_c. The horizontal top and bottom walls are thermally insulated and impermeable. Horizontal parallel plates of height $L/2$ are placed at the center of the cavity. The temperature of the plate maintained at T_h is varying linearly from T_{h1} to T_{h2}. The Cartesian coordinates (x, y) with the corresponding velocity components (u, v) are chosen. The gravity g acts downward normal to the x direction. An inclined magnetic field $\overline{B_0}$ is applied with respect to the coordinate system.

The flow is assumed to be laminar incompressible and the fluid properties are assumed to be constant except the density. The density variation is considered into the account using Boussinesq approximation which can be seen as buoyancy force. Under the above assumption, the governing equations for unsteady natural convection flow using conservation of mass, linear momentum, angular momentum and energy can be written in the non-dimensional form as follows [16,17]:

$$\nabla^2\Psi = -\zeta \tag{1}$$

$$\begin{aligned}\frac{\partial\zeta}{\partial\tau}+J(\Psi,\zeta) &= \Pr(1+K)\nabla^2\zeta-\Pr K\nabla^2 N+Ra\Pr\left(\cos(\gamma)\frac{\partial\theta}{\partial X}-\sin(\gamma)\frac{\partial\theta}{\partial X}\right)\\ &+\Pr Ha^2\left(\sin(\varphi)\cos(\varphi)\frac{\partial U}{\partial X}-\cos^2(\varphi)\frac{\partial V}{\partial X}\right)-\Pr Ha^2\left(\sin(\varphi)\cos(\varphi)\frac{\partial V}{\partial Y}-\sin^2(\varphi)\frac{\partial U}{\partial Y}\right)\end{aligned} \tag{2}$$

$$\frac{\partial N}{\partial\tau}+J(\Psi,N)=\Pr(1+K/2)\nabla^2 N-\Pr(2KN)+\Pr K\left(\frac{\partial V}{\partial X}-\frac{\partial U}{\partial Y}\right) \tag{3}$$

$$\frac{\partial N}{\partial\tau}+J(\Psi,\theta)=\nabla^2\theta \tag{4}$$

$$U=\frac{\partial\Psi}{\partial Y},\; V=-\frac{\partial\Psi}{\partial X} \tag{5}$$

where

$$\zeta = -\frac{\partial U}{\partial Y} + \frac{\partial V}{\partial X} \tag{6}$$

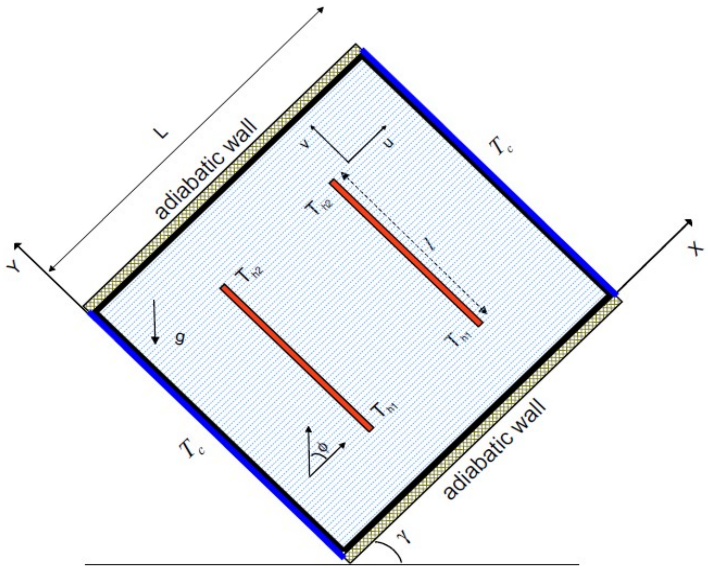

Fig. 1. Physical model and coordinate system

The initial and boundary conditions are

$$\tau = 0: U = V = 0,\ N = 0,\ \theta = 0,\quad \text{for}\ \ 0 \le X \le 1\ \text{ and }\ 0 \le Y \le 1$$

$$\tau > 0: U = V = 0,\ N = 0,\ \theta = 0,\quad \text{for}\ \ X = 0,1\ \text{ and }\ 0 \le Y \le 1$$

$$U = V = 0,\ N = 0,\ \frac{\partial\theta}{\partial Y} = 0,\quad \text{for}\ \ Y = 0,1\ \text{ and }\ 0 \le X \le 1 \tag{7}$$

$$U = V = 0,\ \theta = \begin{cases} 1 + \dfrac{\lambda}{\varepsilon}(1 - 2X) & (\text{at the horizontal paperellel plates}) \\ 1 + \dfrac{\lambda}{\varepsilon}(1 - 2Y) & (\text{at the vertical paperellel plates}) \end{cases}$$

It is noted that for $K = 0$, the above equations identify the classical problem of free convection of a Newtonian fluid in a square cavity. For $K > 0$, represent the micro-polar fluid.

Introducing the following dimensionless variables

$$(X,Y) = \frac{(x,y)}{L},\quad (U,V) = \frac{(u,v)}{\alpha/L},\quad \tau = \frac{t}{L^2/\alpha},\quad \theta = \frac{T - T_c}{\Delta T},$$
$$\Delta T = \frac{T_{h1} + T_{h2}}{2} - T_c,\quad \Psi = \frac{\psi}{\alpha},\quad (\zeta, N) = \frac{(\omega, N')}{\alpha/L^2}, \tag{8}$$

where $Ra = (g\beta L^3 \Delta T)/(\upsilon\alpha)$, Rayleigh number, $Ha = \overline{B_0} L\sqrt{\sigma/\mu}$, Hartmann number, $\Pr = \nu/\alpha$, Prandtl number, $\varepsilon = l/L$ dimensionless length of the plate and $\lambda = (T_{h1} - T_{h2})/(2\Delta T)$ source non-uniformity parameter. The physical quantities of interest are the local Nusselt number (Nu_{local}) and average Nusselt number ($\overline{Nu}$) which are defined as:

$$\overline{Nu} = \int_0^1 Nu\, dX \tag{9a}$$

$$Nu_{local} = -\left.\frac{\partial\theta}{\partial Y}\right|_{Y=0,1} \tag{9b}$$

3. Numerical Approach and Validation

Numerical solutions of the governing equations were obtained using the finite volume method [22]. To approximate the diffusion term in the vorticity and energy equations, the second order central difference scheme is used. Moreover convective terms are carried out by a second order upwind differencing scheme which gives a better solution. For the solution of the vorticity equation, the values of the vorticity at the boundaries are required. For this we employed a second order expression for Ω_w in the form (at the bottom wall)

$$\Omega_w = \frac{\Psi_{i,2} - 8\Psi_{i,1}}{2h^2} \tag{10}$$

by writing the stream function Ψ using Taylor series expansion near the walls. Finally the velocity components at all the grid points were calculated by using the central difference approximations to $U = \partial\Psi/\partial Y$ and $V = -\partial\Psi/\partial X$. The entire procedure was repeated in the successive time levels until θ and Ω converge at a given time level when the following convergence criteria

$$\frac{\left|\Phi_{i,j}^{n+1} - \Phi_{i,j}^{n}\right|}{\left|\Phi_{i,j}^{n+1}\right|} \le 10^{-6} \tag{11}$$

for temperature, vorticity and stream function have been met. In the above expression n represents the time level and Φ represents θ, Ω or Ψ. In order to check on the accuracy of the numerical technique employed for the solution of the problem considered in the present study, it is validated with Aydin and Pop [23] for the average Nusselt number in the presence of micropolar fluid, which is represented in Fig. 2. These results provide confidence in the accuracy of the present work. Following, the case of free convection in two-dimensional square cavity heated from below was considered. The heat source is located centrally on the bottom wall of the cavity. The obtained numerical results were validated against the experimental data presented by Corvaro and Paroncini [24]. Figs. 3 and 4 show the numerical results and experimental results exhibit the similar trends. The computation is carried out for different grids and it is seen that it does not show any significant change after the grid size 81 (see Table 1). Therefore, the numerical solutions are presented with 81 × 81 grid system.

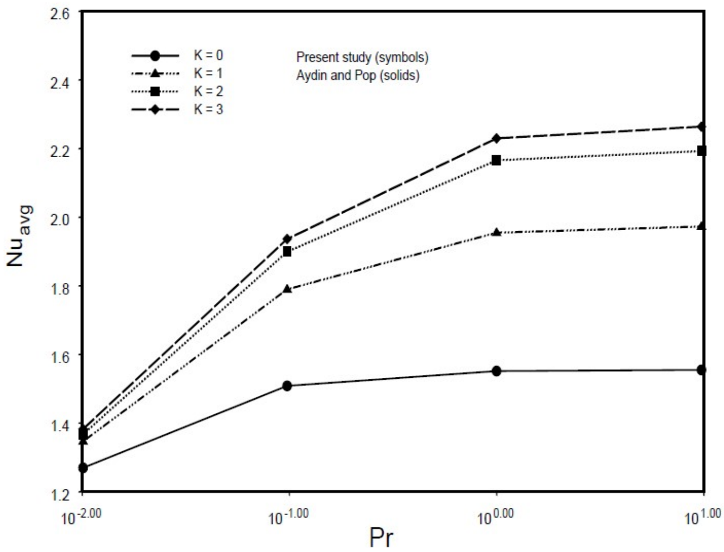

Fig. 2. Average Nusselt number for different values of Rayleigh numbers and vortex viscosity parameter for $Pr = 0.71$ and $n = 0$

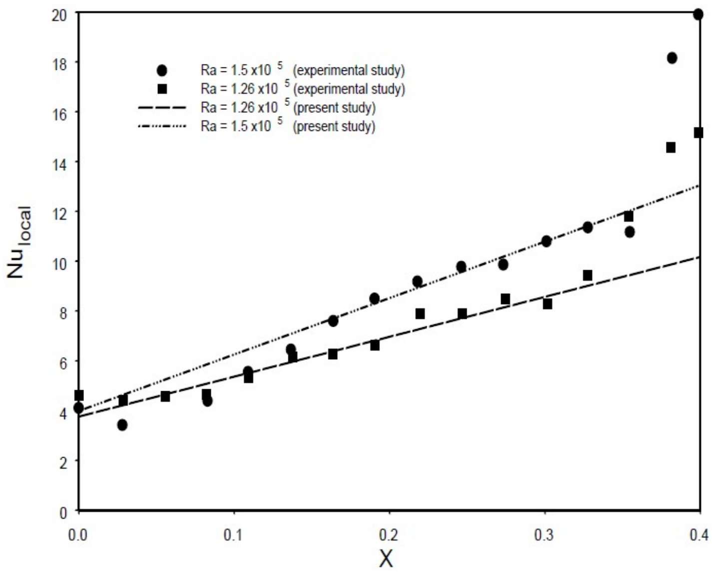

Fig. 3. Local Nusselt number on the heated plate for $\varepsilon = 0.3$

Table 1. Average Nusselt number for different grid systems with Pr = 7.0 , $Ra = 10^5$, Ha=50, $\phi = \gamma = 45^o$, K=1 and $\lambda = 0.0$

Grid size	21×21	41×41	61×61	81×81	101×101	121×121
Nu_{avg}	4.675862	4.409251	4.274421	4.239874	4.213254	4.213124

4. Results and Discussion

In this study, the numerical results show the effects of inclined Lorentz force on the natural convection micropolar fluid in an inclined square cavity in the presence of parallel heat source with various Rayleigh numbers (Ra = 10^3−10^6), Hartmann numbers (Ha = 0−70), inclination angle (γ = 0^o−90^o), orientation angle of magnetic field (ϕ = 0^o − 90^o), vortex viscosity parameter (K = 0 − 3) and non-uniform heating parameter (λ = 0 − 1). The water considered as the working fluid with the Prandtl number Pr = 7.0. The length of the parallel plates are fixed at ε = 0.5. The computational results discussed in the form of streamlines, isotherms, micro-rotation, local Nusselt number and average Nusselt number for the various physical parameters.

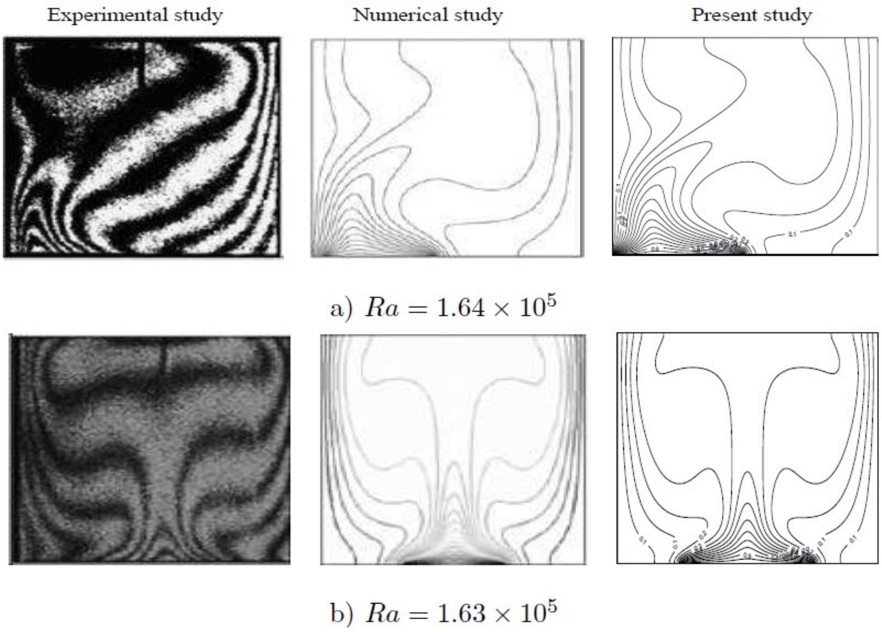

Fig. 4. Isotherms comparison between experimental and present study for a) $\varepsilon = 0.25$ b) $\varepsilon = 0.5$

4.1. Effect of horizontal plates

Fig. 5 shows the streamlines and isotherms for γ = ϕ = 45^o, K = 2 and λ = 0 with different Rayleigh number and Hartmann number. It indicates that the fluid particles observed heat from the heat source and start rising from the bottom to top and then fall down making the recirculation eddies in the cavity. The corresponding isotherms are clustered deeply near the cold walls which state the steep temperature gradients in the vertical direction. The gradient of temperature is generated from the heat source and it forms the two isothermal regions near the left and right walls. Due to the inclined angle, the fluid circulation in the left half of the cavity is steeper than the right half of the cavity. Therefore convection is more pronounced in that region due to the absence of magnetic field. As an increase in Ha, the flow circulation becomes weaker and hence the convection is reduced in the entire cavity. As the value of the Rayleigh number increases, more convection is induced in the cavity due to the parallel heat source and also the vortices increases in its size and strength in the right half of the cavity. The isotherms indicate that the high-temperature gradient occurs at the right half of the cavity. As the Hartmann number increases further, the Lorentz force dominates on the buoyancy force. Therefore strength of the fluid flow and thermal field decrease with an increases in the Hartmann number. The flow intensity and temperature distribution are weakened in the left half of the cavity. This is because the magnetic field effect is more prominent in that region due to the cavity inclination.

Fig. 6 shows the typical contours for the streamlines and isotherms obtained numerically corresponding to the non-uniform heating case for various values of the Hartmann number and Rayleigh number. For Ra = 10^5, it is to be noted that, at low Hartmann number (Ha = 0), the effect of buoyancy force dominates the flow field in the entire cavity. Therefore higher temperature gradients occurred around the parallel heat source. When the magnetic field is imposed on the enclosure, the flow velocity is suppressed owing to the retarding effect of the Lorenz force. So, the convection strength weakens significantly. As Ra increases to Ra = 10^6, streamlines are distorted in shape and the value of the stream function enhances with more energy input to the cavity. The isotherms show the steep temperate gradient around the parallel plates and upper part of the cold walls. In addition, the conduction is restricted to the overall cavity and is dominated by convection. As the magnetic field Ha increases, the flow intensity reduces and the size of the vortex is enlarged in the cavity. This indicates the predominance of the conduction heat transfer mechanism which is due to the suppression of buoyancy force by the viscous force, and particularly by the presence of higher magnetic field.

Ha=0 Ha=30 Ha=70

a) Ra = 10^5

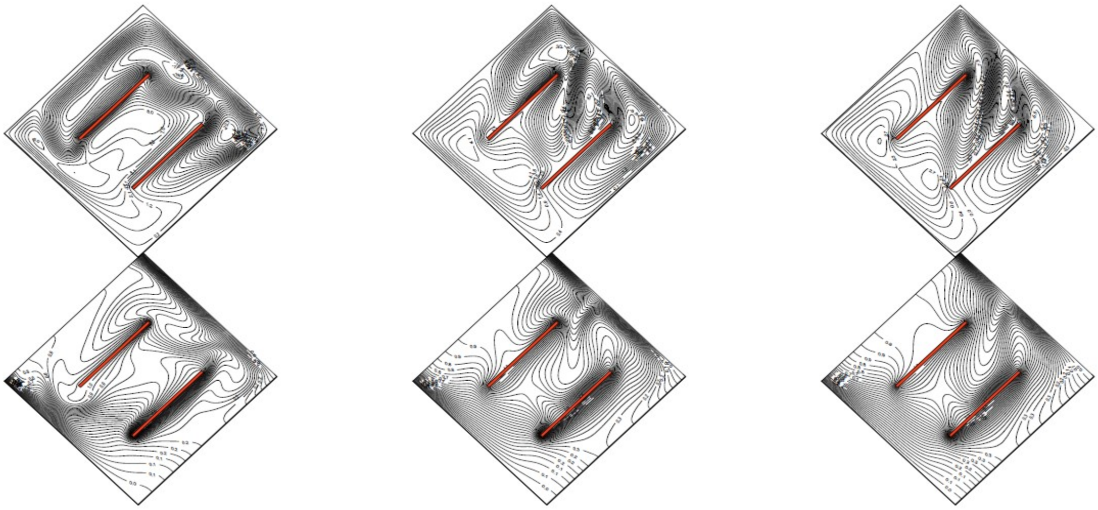

Ha=0 Ha=30 Ha=70

b) Ra = 10^6

Fig. 5. Streamlines (top) and isotherms (bottom) for horizontal plates with $\lambda = 0$, $K = 2$, $\gamma = \phi = 45^o$ and different *Ha* and *Ra*

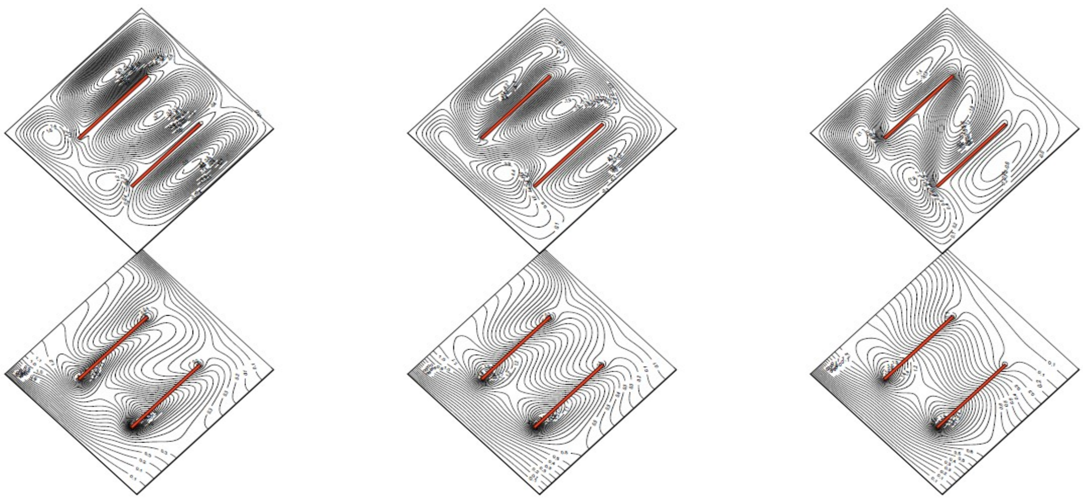

Ha=0 Ha=30 Ha=70

a) Ra = 10^5

Fig. 6. Streamlines (top) and isotherms (bottom) for horizontal plates with $\lambda = 1$, K=2, $\gamma = \phi = 45^o$ and different *Ha* and *Ra*

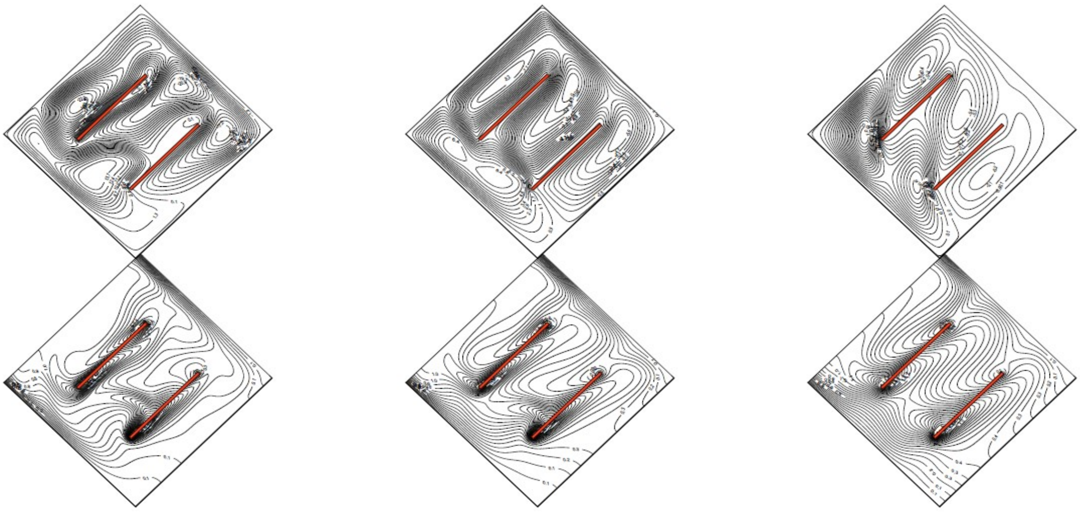

Ha=0 Ha=30 Ha=70

b) Ra = 10^6

Fig. 6. Continued

Fig. 7 displays typical fluid flow, temperature distribution and micro-rotation contours for different non-uniform heating parameters and inclination angle at $Ra = 10^5$, $Ha = 30$, $\phi = 45^o$ and $K = 2$. For $\lambda = 0$, the hot fluid rises from the heat sources and turns to fall along the cold walls forming a clockwise and anti-clockwise rotating cells. The isotherms are more packed around the bottom plate and the top region of the cavity. When the inclination angle changed to $\gamma = 90^o$, the structure of the recirculation cell loses its symmetric pattern. The left vortex increases in its size as well as isotherms more pronounced in the top half of the cavity. This is happens that direction change of the Lorentz force due to the inclination of the cavity. A similar behaviour is also observed for the micro-rotation contours. The streamlines, isotherms and micro-rotation are shown in the Fig. 8 for the non-uniform heating of the parallel plates. It observed from the streamlines the flow intensity is higher and isotherms are more clustered in the left half of the cavity. This reveals that the flow and temperature distribution is more prominent in that region due to the non-uniform heating of the plates. As the inclination angle increases to $\gamma = 90^o$, the circulation splinting into multi cellular patterns and forming two weaker secondary eddies in the top right corner of the cavity. The isotherms in that region are less pronounced because of the weak buoyancy force. The micro-rotation also obeys this behaviour in the entire cavity as well as it is noticed that the micro-rotation is very sensitive about the inclination angle.

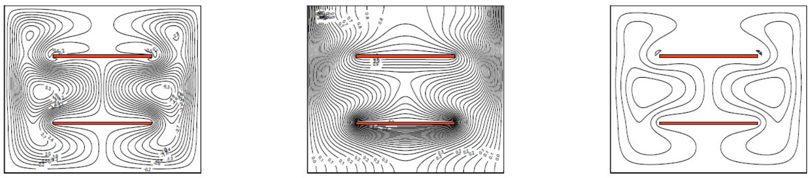

a) $\gamma = 0^o$

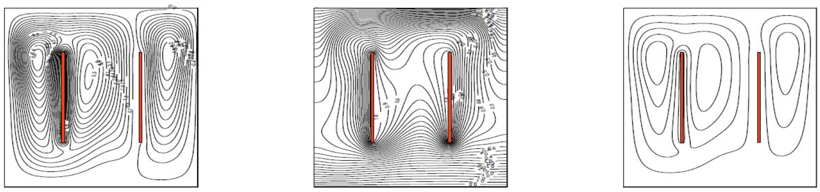

b) $\gamma = 90^o$

Fig. 7. Streamlines (left), isotherms (middle) and micro-rotation (right) for horizontal plates with Ha =30, Ra =10^5, $\phi = 0^o$, $\lambda = 0$, $K = 2$ and different γ

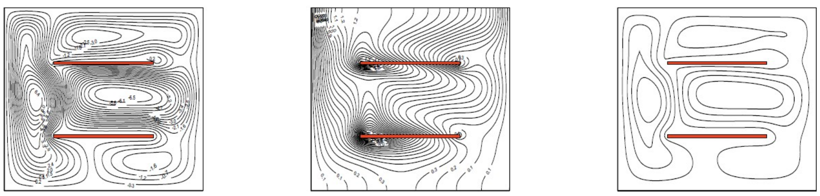

a) $\gamma = 0^o$

Fig. 8. Streamlines (left), isotherms (middle) and micro-rotation (right) for horizontal plates with Ha =30, Ra =10^5, $\phi = 0^o$, $\lambda = 1$, $K = 2$ and different γ

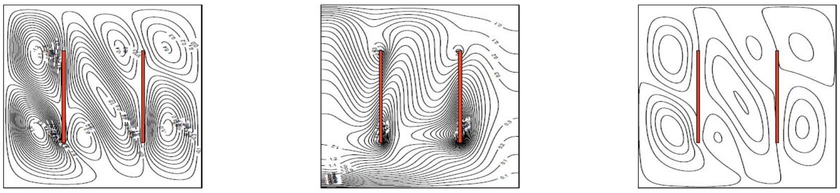

$b)\ \gamma = 90^o$

Fig. 8. Continued

To understand the effect of inclination angle of magnetic field along the left wall is represented in Fig. 9 when the $Ra = 10^5$, $\gamma = 45^o$, $Ha = 50$, $K = 2$ for both uniform and non-uniform heating parameters. The local Nusselt number on the left wall increases and it seems as sinusoidal type of variation is noticeable due to the inclination angle of magnetic field and cavity. It can be clearly seen from the above results that the non-uniform heating of the plate enhances the overall heat transfer rate as to compare with the uniform heating of the plate. The variation of local Nusselt number against the vortex viscosity parameter for both uniform and non-uniform heating of the plate are shown in Fig. 10. A decrease in the local Nusselt number is observed on increasing the vortex viscosity parameter for all values of non-uniformity parameter. The viscous effect is enhanced and the fluid flow is damped thereby reducing the heat transfer rate when K is increased.

The effect of inclination angle and Hartamnn number on the heat transfer is shown in Fig. 11. From the graph it is clear that the increasing values of Hartmann number decreases the heat transfer rate for the both values of non-uniformity parameter. This is due to the fact that presence of magnetic field produces the resistance in the fluid flow thereby decreasing the heat transfer rate. However, it is interesting to note that the average Nusselt number gives the non-monotonic variations for the increasing values of inclination angle. Variation of the average Nusselt number for the different values of Hartmann number and vortex viscosity parameter are shown in Fig. 12. It is noted that the heat transfer rate decreases with an increase of Hartmann number. This due to the convective heat transfer mechanism suppresses when the strength of magnetic field is increased.

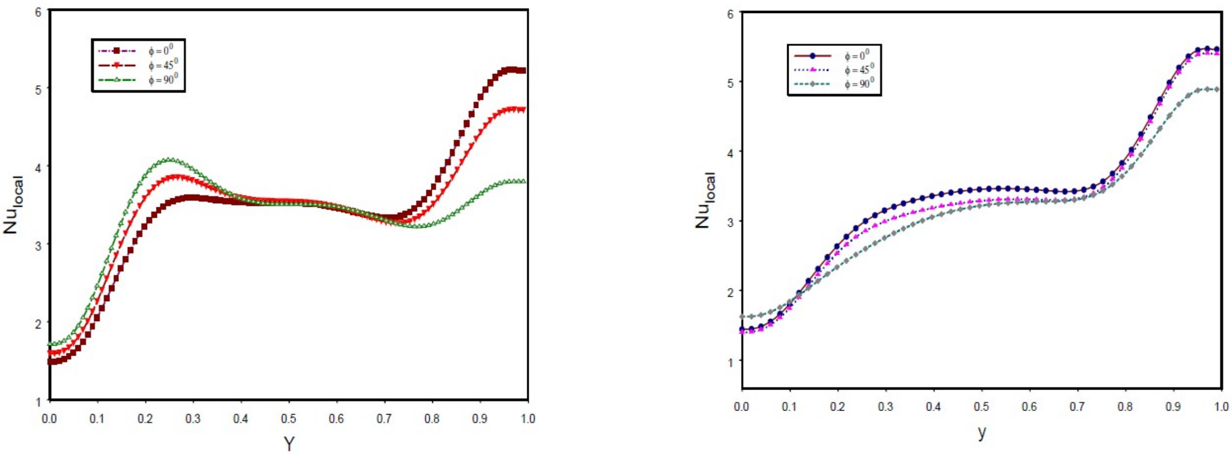

$a)\ \lambda = 0$ $b)\ \lambda = 1$

Fig. 9. Variation of local Nusselt number for the horizontal plates with $Ra = 10^5, Ha = 50, \gamma = 45^o, K = 2$ and inclination angle of magnetic field

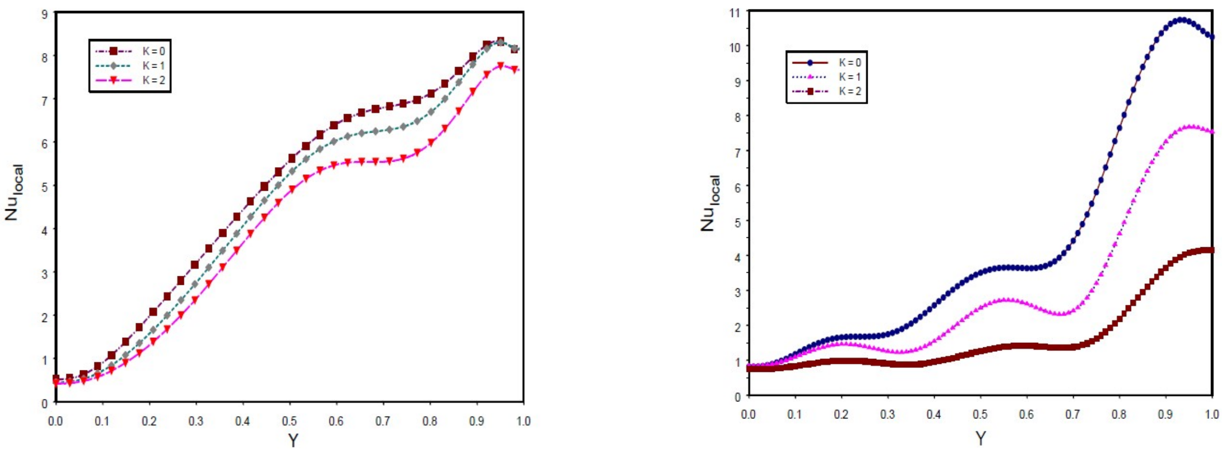

$a)\ \lambda = 0$ $b)\ \lambda = 1$

Fig. 10. Variation of local Nusselt number for the horizontal plates with $Ra = 10^5, Ha = 50, \gamma = 45^o, K = 2$ and different vortex viscosity parameters

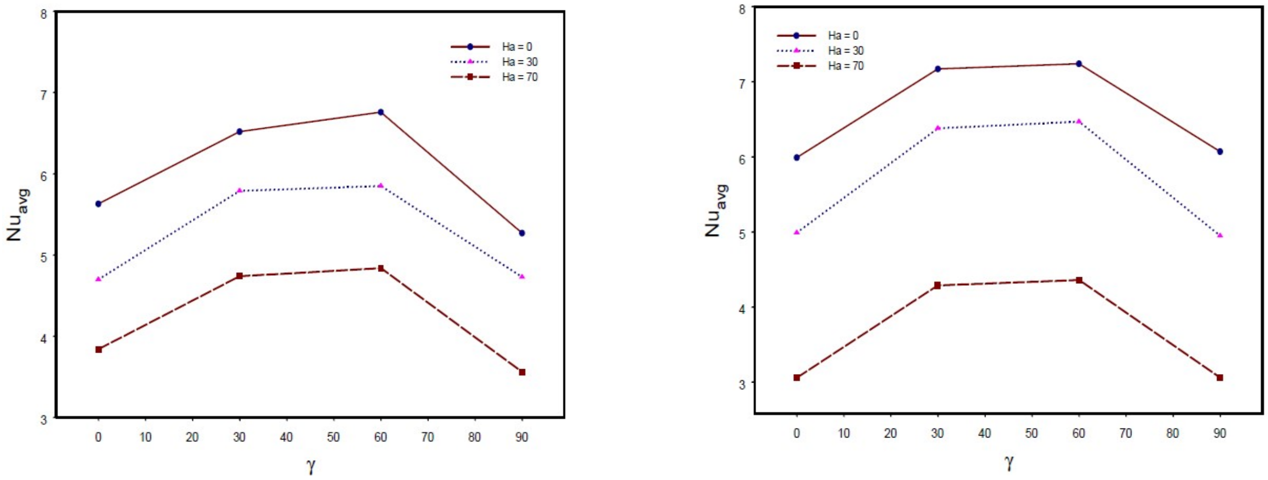

$a)\ \lambda = 0$ $b)\ \lambda = 1$

Fig. 11. Variation of average Nusselt number for the horizontal plates with $Ra = 10^5, \phi = 45^o, K = 2$ and different Hartamnn numbers and inclination angle

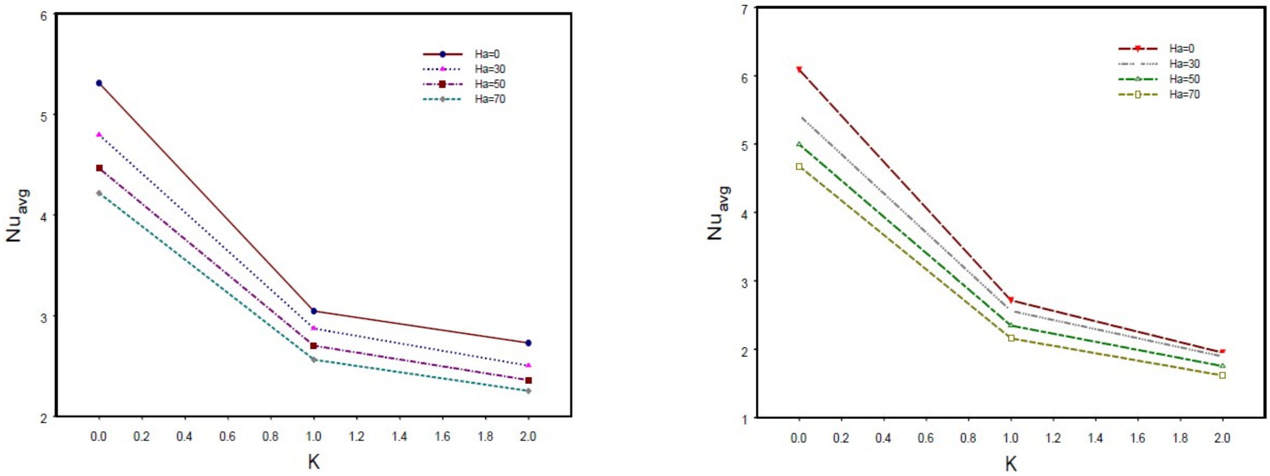

$a)\ \lambda = 0$ $b)\ \lambda = 1$

Fig. 12. Variation of average Nusselt number for horizontal plates with $Ra = 10^5, \gamma = \phi = 45^o$ and different vortex viscosity parameters and Hartmann numbers

Ha=0 Ha=30 Ha=70

a) Ra = 10^5

Fig. 13. Streamlines (top) and isotherms (bottom) for vertical plates with $\lambda = 0$, $K = 2$, $\gamma = \phi = 45^o$ and different Ha and Ra

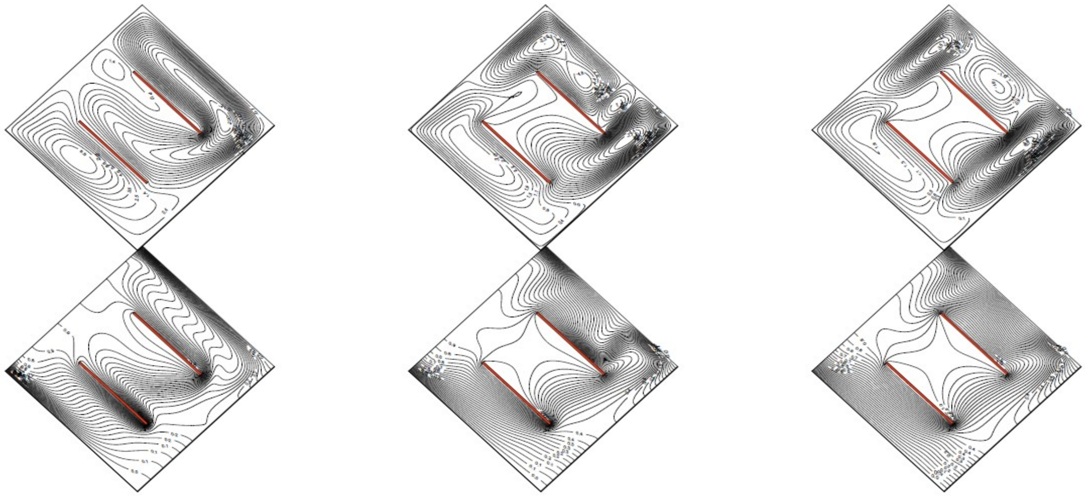

Ha=0 Ha=30 Ha=70

b) Ra = 10^6

Fig. 13. Continued

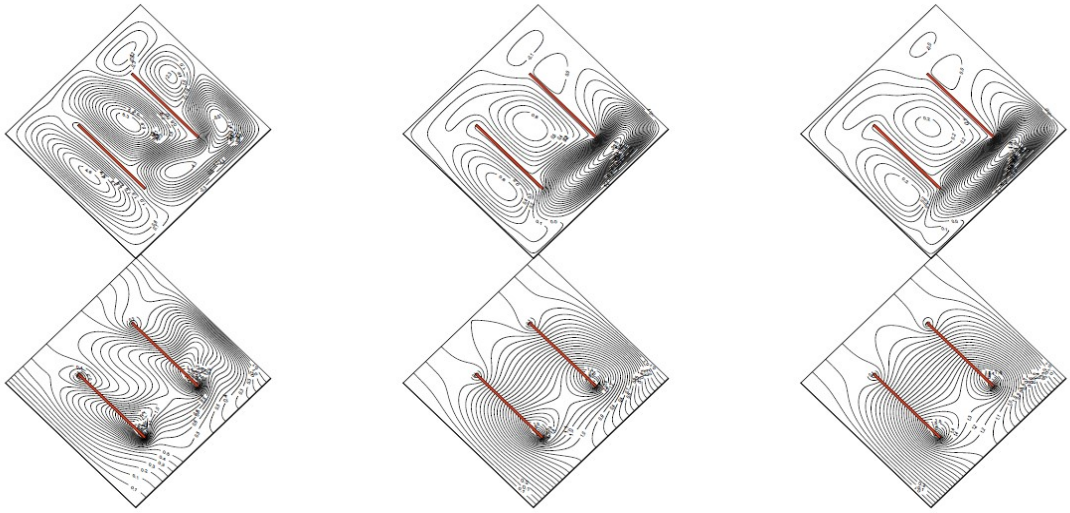

Ha=0 Ha=30 Ha=70

a) Ra = 10^5

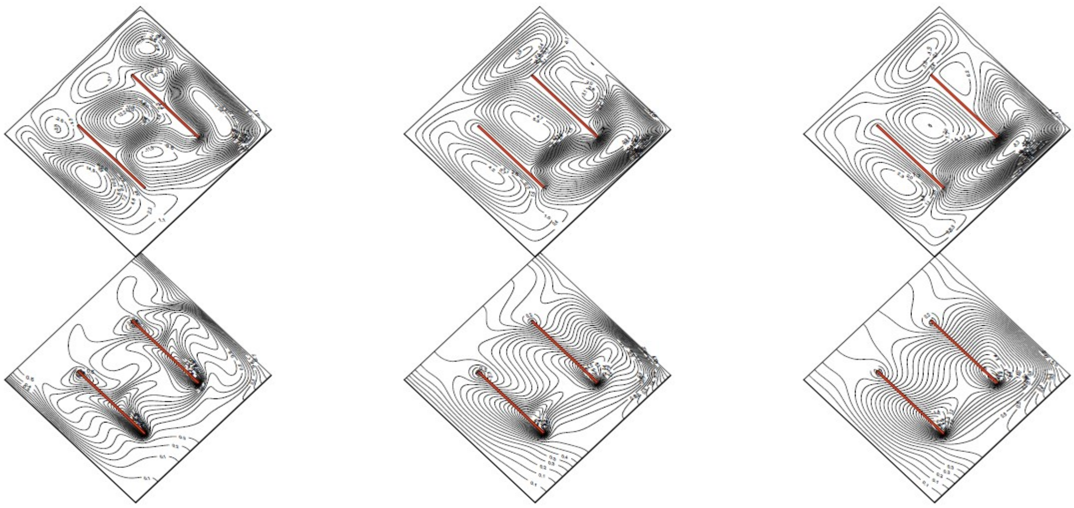

Ha=0 Ha=30 Ha=70

b) Ra = 10^6

Fig. 14. Streamlines (top) and isotherms (bottom) for vertical plates with $\lambda = 1$, $K = 2$, $\gamma = \phi = 45^o$ and different *Ha* and *Ra*

4.2. Effect of vertical plates

Fig. 13 shows an evolution of streamlines and isotherms at $\gamma = \phi = 45^o$, $K = 2$ and $\lambda = 0$ for different values of the Hartmann number and Rayleigh number. It is should be noted that the two anti-symmetric formation of convective cells occupies the entire cavity. The right primary eddy is stronger than the left one due to the presence of inclination angle of the cavity as well as inclined magnetic field. Therefore temperature distribution is stronger on the right half of the cavity as compared to the left half for both the values of the Rayleigh number. When the Hartmann number is absent, the intensity of the fluid flow becomes strong, since the buoyancy force dominates the flow field due to the natural convection. Hence convection heat transfer plays a primary role when the magnetic field effect is negligible which leads to increase the stream function values. The magnetic field taken into the account, the Lorentz force effect becomes higher than the buoyancy force which causes to suppress the flow circulation. Hence, the convection effect reduces significantly. With an increase in the *Ra*, the isotherms are highly concentrated adjacent to the heat sources and their shape is in general curved which indicates that the heat inside the enclosure is transferred due to the natural convection. However, the concentration of the isotherms becomes weakened and isothermal lines become smoother when the Hartmann number is increased.

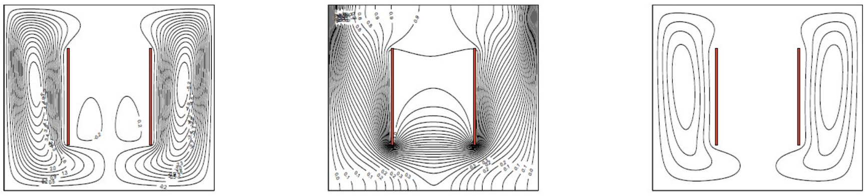

$a)\ \gamma = 0^o$

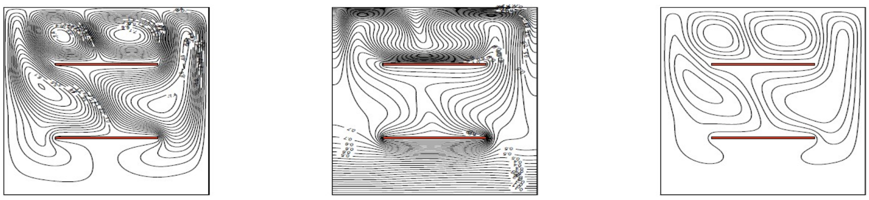

$b)\ \gamma = 90^o$

Fig. 15. Streamlines (left), isotherms (middle) and micro-rotation (right) for vertical plates with Ha =30, Ra =10^5, $\phi = 0^o$, $\lambda = 0$, $K = 2$ and different γ

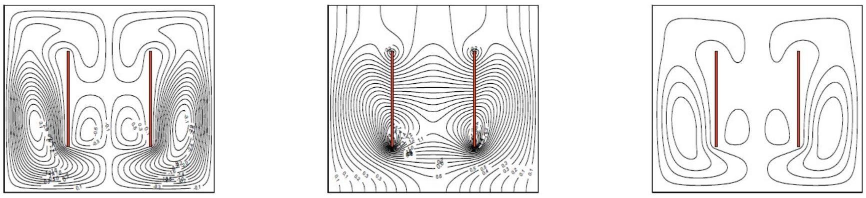

$a)\ \gamma = 0^o$

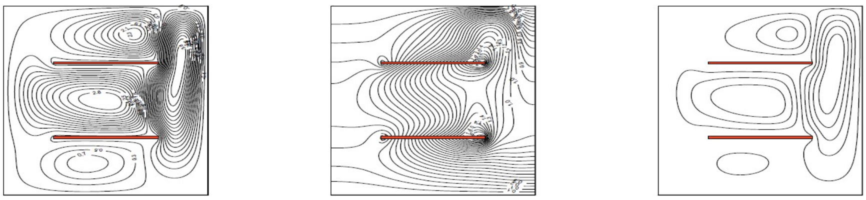

$b)\ \gamma = 90^o$

Fig. 16. Streamlines (left), isotherms (middle) and micro-rotation (right) for vertical plates with Ha =30, Ra =10^5, $\phi = 0^o$, $\lambda = 1$, $K = 2$ and different γ

Fig. 14 shows the fluid flow, temperature distribution and micro-rotation for the different values of *Ha* and *Ra* with $\phi = \chi = 45^o$, $K = 2$ and $\lambda = 1$. When the Hartmann number is not present, the flow patterns consist of multi-vortices that rotate in the clockwise and anti-clockwise directions. The isotherms exposed that the convection mode of heat transfer is observed in the entire cavity. The Hartmann number included in the flow field, the circulation cells reduce in its strength and the conduction regime is more dominant in the cavity. This is due to the presence of magnetic field penetrates in the flow and damped the flow motion. As Rayleigh number increases, the flow strength becomes stronger and the convection mechanism is pronounced in the cavity. Due to the inclined magnetic field and non-uniform heating of the plate, the flow circulation is suppressed and move towards the right bottom corner of the cavity. Therefore, the temperature distribution at the right bottom of the cavity is higher than the other region which leads to high heat transfer is occurred at the right side of the cavity.

Fig. 15-16 show the fluid flow, temperature distribution and micro-rotation for both uniform and non-uniform heating of the plate with Ha = 50, Ra = 10^5, ϕ = 45^o for different values of γ. As seen from the Fig. 15, two eddies are developed inside the cavity and rotating clockwise and anti-clockwise directions. The corresponding isotherms show high temperature gradients near the plates and top half of the cavity when the inclination angle is not present. As the inclination angle is increases, the fluid flow becomes multi cellular pattern and the flow intensity is stronger in the top half of the cavity. Hence, the convection in the upper half of the cavity is more prominent due to the buoyancy force. The angular vorticity is strongly dependent on the inclination angle of the cavity which is observed from the micro-rotation contours. Fig. 16 shows the flow, thermal and micro-rotation fields in the presence of non-uniformly heated vertical plates. The streamlines to higher Rayleigh number exhibit a pair of symmetric and stronger convective patterns in the cavity. The steeper thermal gradients found to be near the bottom of the cavity since the non-uniform heating of the plates, which can be seen from the isotherms. With increase in the inclination angle to ϕ = 90^o, the flow intensity becomes stronger on the right side of the cavity. Therefore, the convective heat transfer is more pronounced in the top right of the cavity. The angular velocity is suppressed and the rotation of the particles moves towards the right side of the cavity when the inclination angle is increased.

Fig. 17 illustrates the variations of local Nusselt numbers on a left wall for various inclination angles of the magnetic field and non-uniformity parameter. This figure shows that the local Nusselt number is dependent of the orientation angle of the magnetic field on both uniform and non-uniform heating. The local Nusselt number increases first and then decreases for all values of ϕ. The similar trend is observed for the non-uniform heating of the plates. The effects of vortex viscosity parameter on the local Nusselt number of the left wall cavity are plotted in Figs. 18 (a) and (b) for different non-uniformity parameter when the remaining parameters are fixed at Ra = 10^6, γ = ϕ = 45^o and Ha = 30. It is found that the high vortex viscosity parameter leads to an increase of the local heat transfer rate whereas the low vortex viscosity parameter reduces the heat transfer rate of the cavity.

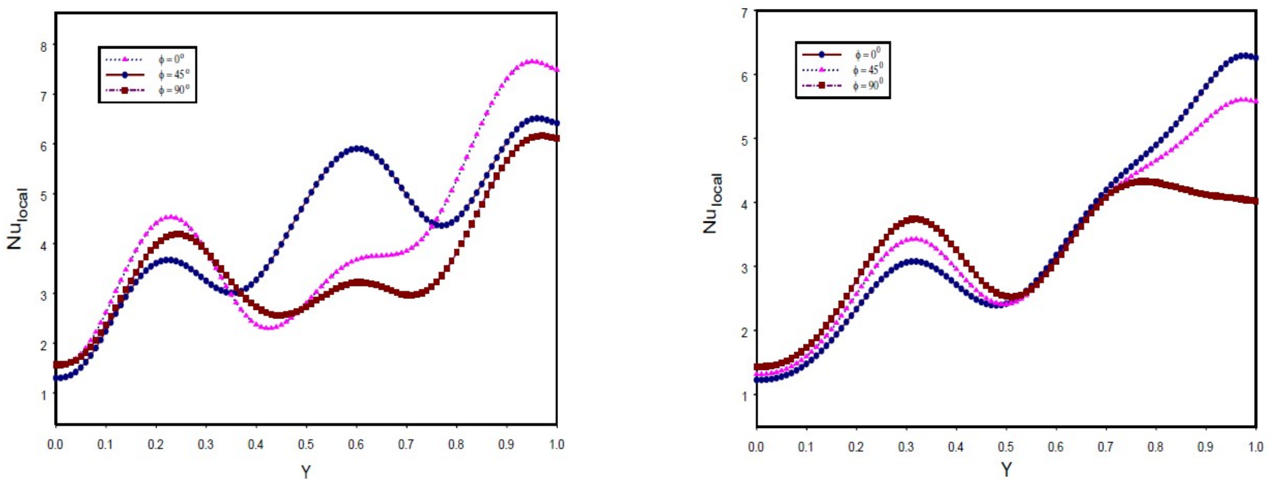

$a)\ \lambda = 0$ $b)\ \lambda = 1$

Fig. 17. Variation of local Nusselt number for the vertical plates with $Ra = 10^5, Ha = 50, \gamma = 45^o, K = 2$ and inclination angle of magnetic field.

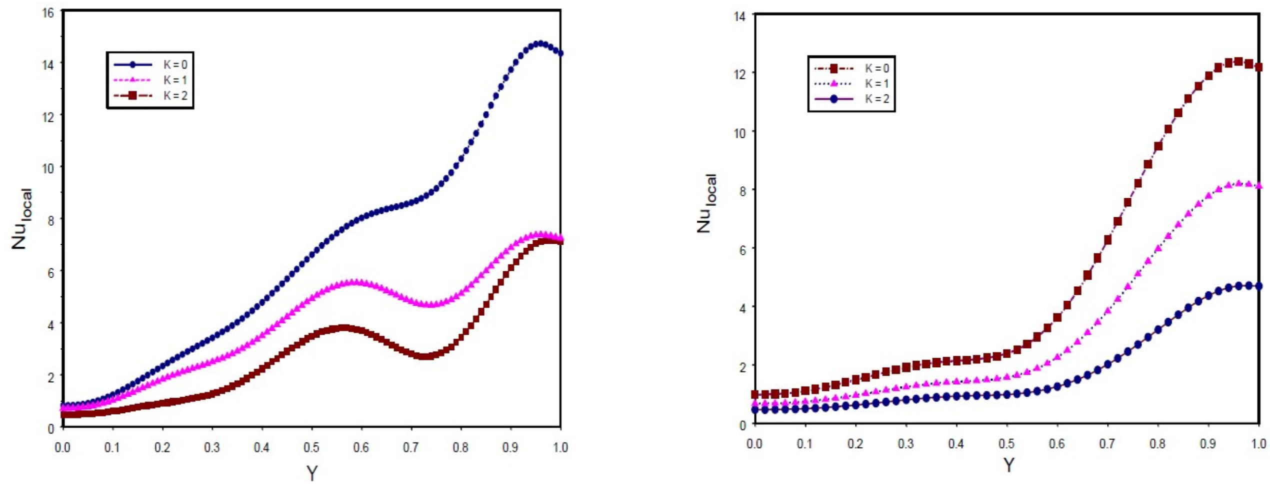

$a)\ \lambda = 0$ $b)\ \lambda = 1$

Fig. 18. Variation of local Nusselt number for $Ra = 10^5, Ha = 30, \phi = \gamma = 45^o$ and different vortex viscosity parameters

Fig. 19 show the effects of Hartmann number and the inclination angle of the cavity with Ra = 10^6, K = 2 and ϕ = 45^o. As seen from the results, the value of the average Nusselt number is highly dependent on the inclination angle. It should be noted that the average Nusselt number attains the maximum value at γ = 60^o for all the values of the Hartmann number. Fig. 20

indicates that the average Nusselt number due to the effect of vortex viscosity parameter and Hartmann number. The average Nusselt number decreases with an increase in Hartmann number at each values of the vortex viscosity parameter for both uniform and non-uniform heating of the plates. This is due to fact that the buoyancy force is reduced when the Hartmann number is increased.

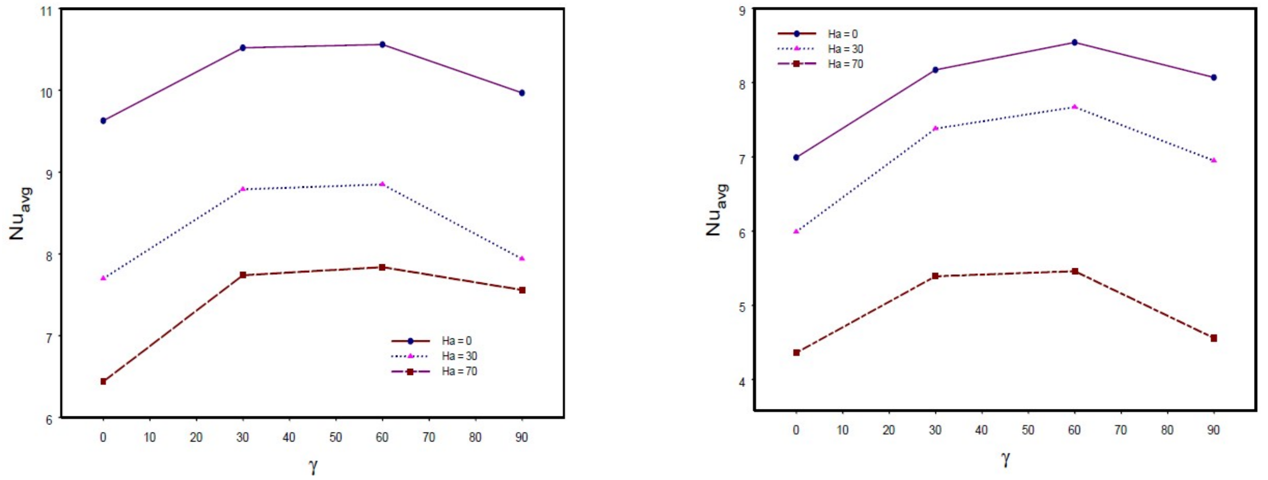

$a)\ \lambda = 0$ $b)\ \lambda = 1$

Fig. 19. Variation of average Nusselt number for vertical plates with $Ra = 10^5, \phi = 45^o, K = 2$ and different Hartamnn numbers and inclination angle

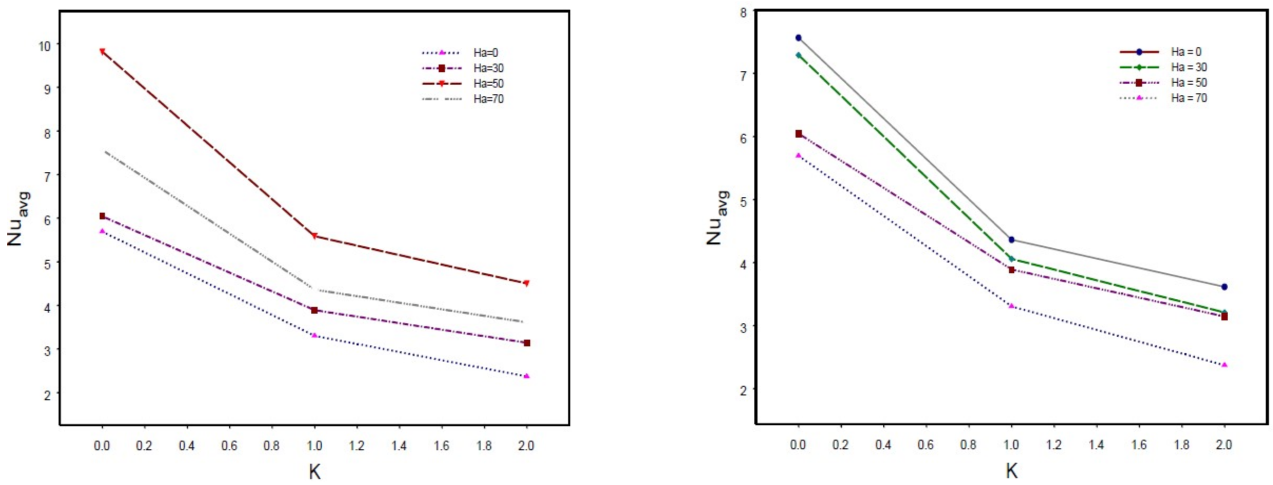

$a)\ \lambda = 0$ $b)\ \lambda = 1$

Fig. 20. Variation of average Nusselt number for vertical plates $Ra = 10^5, \gamma = \phi = 45^o$ with different vortex viscosity parameters and Hartmann numbers

5. Conclusion

Computation on MHD natural convection of micropolar fluid is carried out using finite volume method in an inclined square cavity in the presence of uniform and non-uniform parallel plates. Comparisons with previous published work were performed and found to be in good agreement. From this study, the following conclusions have been drawn.

- The non- uniform heating of the heated plate gives better heat transfer than uniform heating of the plates. It is found that the heat transfer rate is always higher when the plates are placed vertically.
- The strength of fluid circulation is increased when the Rayleigh number increases. However, the magnetic field damps the fluid flow and temperature distributions thereby reducing the fluid velocity and heat transfer rate in the cavity.
- An increase in the inclination angle of the cavity exhibits the non-monotonic variation in the heat transfer rate and makes sinusoidal patterns for all the values of the Hartmann number. The overall heat transfer rate reduces with the orientation angle of the magnetic field.
- It was predicted that the heat transfer obtained on the basis of the Newtonian fluid model gives higher heat transfer than those obtained on the basis of micropolar fluid model.

Conflict of Interest

The author(s) declared no potential conflicts of interest with respect to the research, authorship and publication of this article.

Funding

This research was supported by Basic Science Research Program through the National Research Foundation of Korea (NRF) funded by the Korea Government (No.2017R1A2B2010603). Further, this has been also supported by the program of World Class 300 R&D (S2415805) and by the Program of Business for Cooperative R&D (R0006261, RFP No. 17-102-006) funded by MOTIE.

Nomenclature

L	Length of the cavity (m)	U,V	Dimensionless coordinates
C_p	Specific heat at constant pressure	$J(\varsigma,\Phi)$	N with respect to X,Y
g	Gravitational acceleration	α	Thermal diffusivity (m^2/s)
h	Local heat transfer coefficient (W/(m^2.K))	γ	Inclination angle of the cavity
Nu	Local Nusselt number	ϕ	Inclination angle of the magnetic field
Pr	Prandtl number	β	Thermal expansion coefficient (K^{-1})
q_w	Heat flux (W/m^2)	ν	Kinematic viscosity (m^2/s)
Ra	Raleigh number	θ	Dimensionless temperature
t	Time (s)	ρ	Density (kg/m^3)
T	Temperature (K)	ω	Dimensional vorticity (s^{-1})
x,y	Dimensional coordinates (m)	ψ	Stream function (m^2/s)
X,Y	Dimensional velocity components	Ψ	Dimensionless stream function
u,v	Dimensionless velocity components(m/s)	Ω	Dimensionless voriticity

References

[1] Al-Najem, N.M., Khanafer, K.M., El-Refaee M.M., Numerical study of laminar natural convection in tilted enclosure with transverse magnetic field, *International Journal of Numerical Methods and Heat Fluid Flow*, 8(6), 1998, pp. 651-672.
[2] Ece, M.C., Buyuk, E., Natural-convection flow under a magnetic field in an inclined rectangular enclosure heated and cooled on adjacent walls, *Fluid Dynamic Research*, 38, 2006, pp. 564-590.
[3] Jalil, J.M, Al-Taey K.A., The Effect of Nonuniform Magnetic Field on Natural Convection in an Enclosure, *Numerical Heat Transfer Part A: Applications*, 51(9), 2007, pp. 899-917.
[4] Pirmohammadi, M., Ghassemi, M., Effect of magnetic field on convection heat transfer inside a tilted square enclosure, *International Communications in Heat and Mass Transfer*, 36, 2009, pp. 776-780.
[5] Teamah, M.A, Elsafty, A.F., Massoud E.Z., Numerical simulation of double-diffusive natural convective flow in an inclined rectangular enclosure in the presence of magnetic field and heat source, *International Journal Mechanical Sciences*, 52, 2012, pp. 161-175.
[6] Sivaraj, C., Sheremet, M.A., MHD natural convection in an inclined square porous cavity with a heat conducting solid block, *Journal Magnetism and Magnetic Materials*, 426, 2017, pp. 351-360.
[7] Jetli, R., Acharya, S., Zimmerman, E., Influence of baffle location on natural convection in a partially divided enclosure, Numerical Heat Transfer, 10, 1986 pp. 521-536.
[8] Oztop, H.F., Dagtekin, I., Bahloul A., Comparison of position of a heated thin plate located in a cavity for natural convection, *International Communications in Heat Mass Transfer*, 31, 2004, pp. 121-132.
[9] Kandaswamy, P., Lee, J., Abdul Hakeem, A.K., Saravanan, S., Effect of baffle-cavity ratios on buoyancy convection in a cavity with mutually orthogonal heated baffles. *International Journal Heat and Mass Transfer*, 51, 2008, pp. 1830-1837.
[10] Garoosi, F., Shakibaeinia, A., Bagheri, G., Eulerian-Lagrangian modeling of solid particle behavior in a square cavity with several pairs of heaters and coolers inside, *Powder Technology*, 280, 2015, pp. 239-255.
[11] Eringen, A.C., Theory of micropolar fluids, *Journal Mathematical Mechanics*, 16, 1966, pp. 1-18.
[12] Eringen, A.C., Theory of thermomicrofluids. *Journal Mathematical Analysis and Applications*, 38, 1972, pp. 480-496.
[13]Wang, S.G., Li, T.Y., Hsu, P.T., Natural convection flow of micropolar fluid in a partially divided enclosure, *Acta Mechanica*, 136, 1999, pp. 41-53.
[14] Zadravec, M., Hribersek, M., Skerget, L., Natural convection of micropolar fluid in an enclosure with boundary element method, *Engineering Analysis and Boundary Elements*, 33, 2009, pp. 485-492.
[15] Alloui, Z., Beji, H., Vasseur, P., Double-diffusive and Soret-induced convection of a micropolar fluid in a vertical channel, *Computers & Mathematics with Applications,* 62, 2011 pp. 725-36.
[16] Periyadurai, K., Muthtamilselvan, M., Doh, D.H., Influence of inclined Lorentz force on micropolar fluids in a square cavity with uniform and non-uniform heated thin plate, *Journal of Magnetism and Magnetic Materials*, 420, 2016 pp. 343-355.
[17] Muthtamilselvan, M., Periyadurai, K., Doh, D.H., Convection of micropolar fluid in a square cavity with an inside heater, *AIAA- Journal of Thermophysics and heat Transfer*, 31(4), 2017, pp. 817-831.
[18] Gibanov, N.S., Sheremet, M.A., Pop, I., Free convection in a trapezoidal cavity filled with a micropolar fluid, *International Journal of Heat and Mass Transfer*, 99, 2016, pp. 831-38.
[19] Turkyilmazoglu, M., Mixed convection flow of magnetohydrodynamic micropolar fluid due to a porous heated/cooled deformable plate: Exact solutions, *International Journal of Heat and Mass Transfer*, 106, 2017, pp. 127-134.

[20] Turkyilmazoglu, M., Flow of a micropolar fluid due to a porous stretching sheet and heat transfer, *International Journal of Non-Linear Mechanics*, 83, 2016, pp. 59-64.
[21] Sheremet, M.A., Pop, I, Ishak, A., Time-dependent natural convection of micropolar fluid in a wavy triangular cavity. *International Journal Heat and Mass Transfer*, 105, 2017, pp. 610-622.
[22] Versteeg, H.K., Malalasekera W., *An Introduction to Computational Fluid Dynamic: The Finite Volume Method*. John Wiley and Sons Inc. New York, 1995.
[23] Aydin, O., Pop, I., Natural convection from a discrete heater in enclosures filled with a micropolar fluid. *International Journal Engineering Science*, 43, 2005, pp. 1409-1418.
[24] Corvaro, F., Paroncini, M., Experimental analysis of natural convection in square cavities heated from below with 2D-PIV and holographic interferometry techniques, *Experimental Thermal Fluid Science*, 31, 2007, pp. 721-739.